Binary-encounter electrons observed at 0° in collisions of 1–2-MeV/amu H^+, C^{6+}, N^{7+}, O^{8+}, and F^{9+} ions with H_2 and He targets

D. H. Lee, P. Richard, T. J. M. Zouros,* J. M. Sanders, J. L. Shinpaugh, and H. Hidmi
J. R. Macdonald Laboratory, Kansas State University, Manhattan, Kansas 66506
(Received 31 July 1989; revised manuscript received 21 December 1989)

The energy distribution of binary-encounter electrons (BEE) produced in collisions of 1–2 MeV/amu H^+ and bare C, N, O, and F ions with H_2 and He gas targets is reported at 0° with respect to the beam direction. These electrons result from ionization of the target due to hard collisions with the projectile and can thus be considered to be produced in a process analogous to elastic scattering of a free electron from a highly charged ion. An impulse-approximation (IA) model has been developed to describe this process in which "quasifree" target electrons undergo 180° Rutherford scattering in the projectile frame. The measured BEE double-differential production cross sections for bare ions were well described by this model and were found to scale with Z_p^2 and $E_p^{-(\sim 2.6-2.7)}$ where Z_p and E_p are the charge and energy of the projectile, respectively. An energy shift of the BEE below $4t$, where t is the cusp electron energy, is observed and is also predicted by the IA treatment. A plane-wave Born approximation (PWBA) calculation for BEE production is also found to be in overall agreement with our data. However, the energy shift of the BEE peak could not be fully accounted for within this PWBA calculation.

I. INTRODUCTION

Binary-encounter electrons[1–3] (BEE) are target electrons ionized through direct, hard collisions with energetic projectiles, giving rise to a broad energy distribution. Using elastic two-body collision dynamics for heavy-ion impact on a *free* electron, the energy of the recoiling electron can be shown to equal $4t\cos^2\theta_{\rm lab}$ and is known as the BEE peak energy.[2,3] The cusp electron energy is given by $t=(m/M_p)E_p$, where m/M_p is the electron-to-projectile mass ratio, E_p is the projectile energy, and $\theta_{\rm lab}$ is the laboratory electron observation angle with respect to the beam direction. Thus for zero-degree measurements ($\theta_{\rm lab}=0°$) the BEE peak energy should be at $4t$.

The production of BEE has been studied using H and He projectiles,[4–11] however, to our knowledge, only a few measurements using heavy-ion projectiles have been reported[1,12] and none at 0°. A detailed understanding of BEE can be useful in the study of characteristic K Auger electron spectra in heavy-ion–atom collisions, since BEE production is often the dominant component of such spectra and can interfere with coherent Auger electrons, as, for example, in resonant transfer excitation followed by Auger decay (RTEA).[13,14] Thus it is important to have a good quantitative model of BEE production that can give the correct projectile E_p and Z_p dependences, as well as a good description of projectile screening[3,15,16] and target electron binding effects.

In this paper, we report on the production of binary-encounter electrons at 0° with respect to the beam direction in energetic 1–2-MeV/amu collisions of *bare* ions with H_2 and He targets. By utilizing bare projectiles we eliminate complications due to possible screening effects,[3,15] and by using two-electron targets we focus on the BEE production for only the K shell. At the rather high collision energies involved in this study, both the impulse approximation[17] (IA) and the plane-wave Born approximation[18] (PWBA) should provide a good description of BEE production. Thus by measuring double-differential cross sections (DDCS) of electron production, in both electron energy and solid angle, we can provide a stringent test of both the IA and PWBA treatments of energetic ion-atom collisions.

In particular, we have developed an IA model in which BEE production at zero degrees can be viewed from the projectile frame, essentially as 180° Rutherford scattering of a "quasifree" target electron by the projectile ion. Upon integrating the Rutherford cross section over the incoming electron's momentum distribution due to its orbital motion around the target nucleus (Compton profile) and correctly accounting for its binding energy, we find that the predicted DDCS are in excellent agreement with our data, particularly in the case of the H_2 targets, over the whole range of collision energies and projectile species studied here. The PWBA DDCS are also found to be in overall agreement with the results of the IA and experiment for H_2 targets. However, the BEE peak, observed to be shifted towards lower electron energies (see Fig. 1) from $4t$, is in better agreement with our IA formula than with the PWBA.

Based on the excellent systematic agreement between the IA and the measured DDCS for projectiles ranging from protons to F^{9+}, it was decided that our IA formula for BEE production could be used to provide a direct and accurate *in situ* absolute efficiency normalization (calibration) of our electron spectrometer in the electron energy range of 1–5 keV. This eliminates the extrapolation of the efficiency derived from the normalization to known Ne target K Auger electron cross sections[19,20] (Auger energy about 0.8 keV) produced by proton impact.

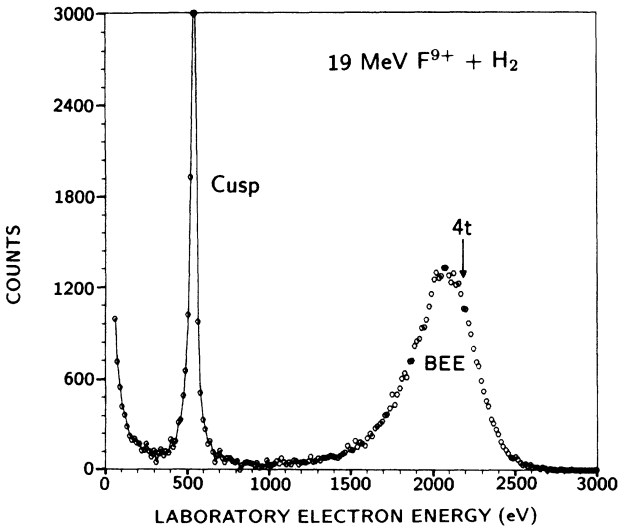

FIG. 1. Electron-energy spectrum for the collision of 19-MeV $F^{9+}+H_2$ observed at 0° showing the cusp and binary encounter peaks. The cusp, not shown in its full height, at energy t is about 5.5 times higher than the binary encounter peak. The maximum of the binary-encounter peak appears at an energy slightly lower than $4t$ (arrow).

In addition, BEE studies of this kind lay the foundation for the investigation of more complicated multielectron-ion-atom collision systems[16] and possibly provide an alternative way (other than the more direct but difficult electron-ion crossed-beam experiments) to study multielectron ion-electron scattering.

II. EXPERIMENT

The experiment was performed using highly charged ion beams produced by the Kansas State University tandem Van de Graaff accelerator. A 0° tandem 45° parallel-plate electron spectrometer[21] with a channeltron detector was used to analyze the energy of electrons produced in the collisions. The performance of this spectrometer has already been reported in measurements of *KLL* Auger electrons used in state-selective determinations of absolute cross sections of various ion-atom collision processes.[21–23]

The electron spectra were obtained with 2.8% full width at half maximum (FWHM) energy resolution without any electron-energy retardation. The binary-encounter electrons were recorded under single-collision conditions found to be valid for target gas pressures less than 80 mTorr in a 10-cm-long gas cell. The gas cell was doubly differentially pumped,[21] so that the chamber pressure could be maintained below 0.01 mTorr at typical gas cell pressures of 40 mTorr. A shielded Faraday cup was used to measure the beam current, which normalized the electron count for each electron energy channel. Partial charge neutralization of the projectile beam due to electron capture in passing through the target gas, which could give rise to erroneous beam integration, was found to be negligible for the collision systems studied here.[24]

Considerable care was taken in reducing the beam-induced background by carefully collimating the beam. Such a background is produced mainly by electrons scattered by the beam at the edges of the spectrometer slits and gas-cell apertures and can be a large source of error at 0° observation. This beam-induced electron background was directly determined by taking an electron spectrum without gas in the target cell. Around the BEE peak, this background could be reduced to less than a few percent of the true counts and was subtracted with small error.

Figure 1 shows a representative electron spectrum for a collision of 19-MeV $F^{9+}+H_2$. The BEE peak is the broad structure at the high-energy side of the spectrum. We note that for this relatively high collision energy, the BEE peak is well separated from the cusp.

III. CALCULATION OF DOUBLE DIFFERENTIAL CROSS SECTIONS

Figure 2 shows a schematic diagram of the relevant kinematic quantities associated with the production of BEE in the "projectile" frame. In this figure, the z axis is defined along the projectile velocity $\mathbf{V}_p$, $\mathbf{s}$ is the cusp momentum ($m\mathbf{V}_p$), and $\mathbf{p}_i$ is the target-electron's orbital momentum. The BEE production cross section can be evaluated in the projectile frame within the impulse-approximation treatment[17] as follows:

$$\left[\frac{d\sigma}{d\Omega}\right]_{BEE}=\sum_i \int \left[\frac{Z_p^2 e^4}{16E^2\sin^4(\theta/2)}\right]|\psi_i(\mathbf{p}_i)|^2 d^3p_i \ . \quad (1)$$

The expression within the large parentheses on the right-hand side of Eq. (1) is the Rutherford scattering cross section of a free electron by a bare projectile ion. $Z_p e$ is the projectile nuclear charge for the case of a bare projectile. For the 0° BEE measurement, the electron scattering angle is $\theta=180°$ in the projectile frame. The target-electron momentum wave function is given by $\psi_i(\mathbf{p}_i)$, where the subscript i refers to the ith target electron. E is the electron energy in the projectile frame.

Including the target ionization energy E_I, from energy conservation considerations, E can be expressed as

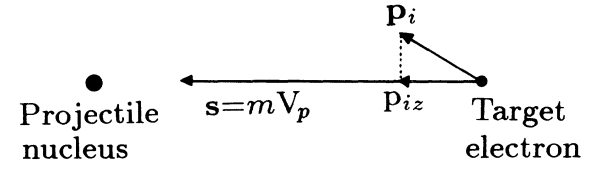

FIG. 2. Schematic diagram of the kinematics of a target electron in a binary-encounter collision with a projectile as seen from the projectile frame. $\mathbf{s}\equiv m\mathbf{V}_p$ is the cusp momentum, where m is the electron mass and $-\mathbf{V}_p$ is the projectile velocity. $\mathbf{p}_i$ and p_{iz} are the target-electron's orbital momentum and its component along the beam axis (z axis), respectively. In this reference frame the target electrons undergo 180° Rutherford scattering from the projectile nucleus and give rise to the BEE observed at 0° in the laboratory frame.

$$E=(\mathbf{s}+\mathbf{p}_i)^2/2m-E_I$$
$$=(s^2+2sp_{iz}+p_{iz}^2+p_{iy}^2+p_{ix}^2)/2m-E_I\ . \quad (2)$$

Since the scattering takes place in a plane, the component of $\mathbf{p}_i$ perpendicular to the plane, p_{iy}, is identically zero, and p_{ix}, which is perpendicular to the cusp momentum $\mathbf{s}$, is neglected, since $(p_{ix}/s)^2 \ll 1$ for fast collisions. For example, in 1-MeV/amu projectile-ion impact, $(p_{ix}/s)^2 \simeq 0.03$ and 0.07 for the most probable value of $\mathbf{p}_i$ set equal to p_{ix} for H_2 and He targets, respectively. We note that $(p_{iz}/s)^2$ is also small for most momentum components and could be neglected, however, it is not necessary to do so for the separation of variables required in the utilization of the Compton profile $J(p_z)$ [see Eq. (5) below]. This differs from Brandt's "linearized" RTE-IA treatment[17] where all quadratic terms and E_I are neglected. It is thus expected that the present model will give improved agreement with the observed BEE spectrum at the low energy wing of the BEE peak, where the large momentum components play an increasingly important role. This effect will be more pronounced for atoms with broader Compton profiles, as in the case of He compared to H_2.

Defining the cusp energy $t\equiv s^2/2m$, the reduced momentum $r\equiv p_{iz}/s$, and the reduced ionization energy $\lambda\equiv E_I/t$, the electron energy E is given within the approximation above by

$$E=t[(1+r)^2-\lambda]\ . \quad (3)$$

Introducing the Compton profile $J(p_z)$ and using Eq. (3), one obtains

$$\left[\frac{d\sigma}{d\Omega}\right]_{\rm BEE}=\int\frac{Z_p^2e^4sJ(p_z)}{32t^3[(1+r)^2-\lambda]^2(1+r)}dE\ , \quad (4)$$

where

$$J(p_z)=\sum_i\int\int dp_{ix}dp_{iy}|\psi_i(\mathbf{p}_i)|^2\ . \quad (5)$$

Experimentally determined[25] Compton profiles were used for both H_2 and He target electrons in the ground state. Thus, the integrand in Eq. (4) is the DDCS for BEE production at 180° in the projectile frame. Therefore,

$$\left[\frac{d^2\sigma}{dE\,d\Omega}\right]_{\rm BEE}=\frac{\sqrt{2}Z_p^2J(p_z)a_0^2}{32\varepsilon_0t^{2.5}[(1+r)^2-\lambda]^2(1+r)}\ , \quad (6)$$

where t and p_z are now in atomic units, and a_0 and ε_0 are the Bohr radius and the atomic unit of energy.

In order to compare with theory, the experimental DDCS and electron energies are transformed from the laboratory to the projectile frame, using[10,26]

$$\left[\frac{d^2\sigma}{dE\,d\Omega}\right]_{\rm BEE}=\left[\frac{d^2\sigma}{dE\,d\Omega}\right]_{\rm BEE}^{\rm lab}\sqrt{E/E_{\rm lab}} \quad (7)$$

and for $\theta=180°$

$$E=(\sqrt{E_{\rm lab}}-\sqrt{t}\,)^2\ , \quad (8)$$

$E_{\rm lab}$ being the laboratory electron energy.

IV. DATA ANALYSIS

A. Determination of the cusp energy t

The cusp energy t, required in Eqs. (6) and (8), was determined experimentally by directly measuring its value in the electron spectrum. This determination of t has been found to be a convenient and reliable way[27] of measuring the actual projectile velocities to within 0.1%, particularly for highly charged ions obtained by poststripping projectile ions of a lower charge state, a process which results in a small but observable energy loss of the beam as it traverses the stripper foil ($\sim$10 μg/cm^2). The experimentally determined values of t are listed in Table I together with t_0, the cusp energy derived from E_p as determined by the accelerator calibration.

TABLE I. Measured cusp energies t and observed energy shifts $\Delta E_{\rm lab}\equiv 4t-E_{\rm lab}^{\rm max}$ (see text), for various projectile and target species. E_p is the projectile energy determined from the accelerator calibration, t_0 is the cusp energy derived from E_p, and $E_{\rm lab}^{\rm max}$ is the laboratory electron energy at the maximum of the BEE peak. Experimental uncertainty on t is about $\pm$2 eV and on $\Delta E_{\rm lab}$ about $\pm$8 eV.

Projectile	E_p (MeV/amu)	t_0 (eV)	t (eV)	$\Delta E_{\rm lab}(H_2)$ (eV)	$\Delta E_{\rm lab}$(He) (eV)
F^{9+}	1.00	549	545	96	186
	1.25	686	682	94	178
	1.50	823	820	93	174
	1.75	960	957	92	171
	2.00	1097	1097	92	169
O^{8+}	1.50	823	820	93	
N^{7+}	1.50	823	823	93	
C^{6+}	1.50	823	823	93	
H^+	$\sim$1.5[a]	$\sim$820[a]	800[b]	37	82
	2.00	1097	1085[b]	19	68

[a]Projectile energy was only approximately known.
[b]1.7% larger values of t were required in the IA and PWBA calculations in order to get agreement with data.

B. Determination of the DDCS and the spectrometer efficiency

The experimental DDCS for electron production in ion-atom collisions, in general, can be obtained from the following well-known expression:[28,29]

$$\left[\frac{d^2\sigma}{dE\,d\Omega}\right]^{\text{lab}}_{\text{expt}} = \frac{Y}{NnlA\Omega\Delta E_{\text{lab}}\eta(E_{\text{lab}})}\ , \tag{9}$$

where Y and N are, respectively, the number of electrons and projectiles counted per electron energy, n is the target number density, l is the length of the gas cell, $\Delta\Omega$ is the effective solid angle, ΔE_{lab} is the spectrometer acceptance energy at electron energy E_{lab}, and $\eta(E_{\text{lab}})$ is the overall spectrometer efficiency.

The efficiency $\eta(E_{\text{lab}})$ is the product of the spectrometer transmission, the channeltron detection efficiency, and other possible factors. Channeltron detection efficiencies have been found to range,[30–32] depending on the experimental setup, from 20% to 100% over the 1–5-keV electron-energy range of interest in this study. In view of these difficulties, $\eta(E_{\text{lab}})$ is determined using our measured electron yields [see Eq. (9)] and the calculated IA-DDCS [see Eq. (6)], at the BEE peak, at each collision energy of the $F^{9+}+H_2$ system. The values of $\eta(E_{\text{lab}})$ determined by this method are given in Fig. 3. Also shown in Fig. 3 is the value of $\eta(E_{\text{lab}}\approx 800\text{ eV})$ determined from the measured 3-MeV H^++Ne K Auger yields normalized to the published[19] cross section. In view of the simple nature of the BEE process, we have selected and used the BEE-IA normalization to test the systematics of BEE production given below.

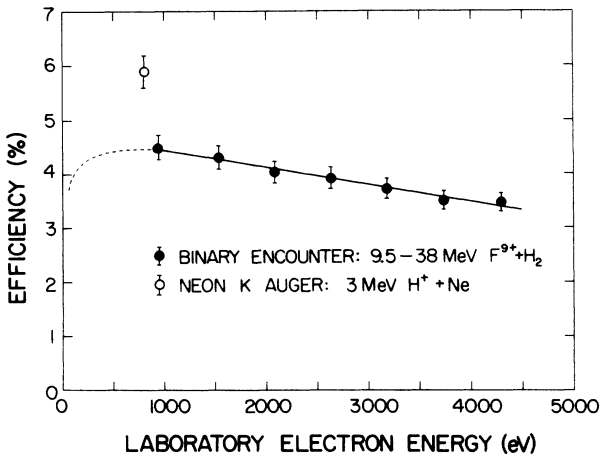

FIG. 3. Overall absolute spectrometer efficiency $\eta(E_{\text{lab}})$ plotted as a function of the laboratory electron energy E_{lab}. The solid line was interpolated using the data points (closed circles) obtained by normalizing the $F^{9+}+H_2$ BEE yields to the IA calculation (see text). The dashed line was extrapolated using the results of Ref. 32. The open circle is the efficiency measured using the known Ne target K Auger cross section (Ref. 19) at $E_{\text{lab}}\approx 800$ eV for 3-MeV H^++Ne collisions. The error bars are calculated from statistics alone. The Ne K Auger data has an overall absolute uncertainty of 20% (Ref. 19).

V. RESULTS AND DISCUSSION

Figure 4 shows the projectile-frame DDCS for collisions of F^{9+} with H_2 and He for three different collision energies. Only the electron yields whose laboratory energies are greater than the cusp electron energy (see Fig. 1) are transformed into the projectile frame, since electrons whose laboratory energies are smaller than the cusp energy are not included in the IA model. The spectrum reflects primarily the underlying Compton profile of the target electrons. We compare this data to the IA model [see Eq. (6)] (solid line) and the PWBA calculation (dashed line).

The overall agreement between the data and the IA is good except in the very-low-electron-energy region, corresponding to electrons with p_{iz} nearly equal and opposite to the cusp momentum, s, for which the impulse approximation approaches the limit of its validity. The combination of the Compton profile and the E^{-2} energy dependence of the Rutherford cross section results in an electron-energy distribution asymmetrically skewed to lower electron energies. The binding energy of the target electron further shifts the energy distribution to even lower energies. These shifts are more pronounced in He than in H_2 targets due to the broader Compton profile and the larger binding energy of He. Therefore, as seen in Fig. 4, the BEE peak is not found at t in the projectile frame ($4t$ in the laboratory frame), as it would if it arose from collisions with truly free electrons (see the vertical arrows in Figs. 1 and 4).

The origin of the BEE energy shift and its asymmetry is investigated in more detail in Fig. 5, where we compare four different calculations with our measurements. The dot-dashed line is the Compton profile[25] for either H_2 or He targets centered at $t-E_I$ in the projectile frame. The solid line is the IA calculation with $E_I=15.5$ and 24.5 eV for the H_2 and He targets, respectively. The dotted line is the IA calculation with $E_I=0$. The dashed line is the PWBA calculation.[18] As observed, around the BEE peak, the PWBA calculation is seen to give the same result as the IA with $E_I=0$ for 1–2-MeV/amu $F^{9+}+H_2$ collisions. The BEE energy shift below $4t$, defined as $\Delta E_{\text{lab}}\equiv 4t-E_{\text{lab}}^{\max}$, was found to vary between ~92–96 eV for H_2 and ~169–186 eV for He targets, in collisions with heavy projectiles (see Table I for details). $E_{\text{lab}}^{\max}$ is the laboratory energy at the maximum of the BEE energy distribution, and was extracted by fitting the data by the IA [see Eq. (6)]. The energy shift ΔE_{lab} becomes smaller at higher projectile energies due to the Rutherford scattering E^{-2} energy dependence. It is interesting to note that the energy shift for protons was smaller than that for the heavy projectiles and could not be fully accounted for, by either the IA or the PWBA treatments, for reasons not yet understood.

The PWBA DDCS were obtained by integrating the analytic expression given in Rudd and Macek[18] over the momentum transfer. In this formulation, the initial state of the target is described by hydrogenic $1s$ wave functions with an effective charge equal to the square root of the binding energy in atomic units.[18] This expression, valid for ionization of a target atom by protons, was general-

ized to treat other bare ions by multiplying the proton results by Z_p^2. In Fig. 6 we compare results from 1.5-MeV/amu H^+ on H_2 and He. Included as an insert is a comparison of the data for 1.5-MeV/amu H^+ and F^{9+} on He. The dash-dotted line is the H^+ data multiplied by Z_p^2 ($=81$). As seen, the Z_p^2 scaling works well only around the BEE peak. The same Z_p^2 scaling trend was observed for the 2-MeV/amu data.

We see that the agreement between the data and the PWBA is also good around the BEE peak for F^{9+} collisions with H_2, but becomes worse for collisions with He (see Fig. 4). In Fig. 4 the energy shift of the BEE peak is not as well accounted for by the PWBA as it is by the IA model. Nevertheless, both IA and PWBA give similar results once the DDCS are integrated over the range of the BEE peak.

In order to test the Z_p dependence of the BEE production more systematically, various bare ions, F^{9+}, O^{8+}, N^{7+}, and C^{6+}, as well as protons were used as projectiles in collisions with H_2 targets at 1.5 MeV/amu. The BEE DDCS for each projectile is compared to the full IA (solid lines) in Fig. 7. The absolute single differential cross section $d\sigma/d\Omega$ at $\theta=180°$ ($\theta_{lab}=0°$) was extracted for each projectile by fitting the experimental DDCS with the IA and then integrating over the BEE peak. The resulting cross sections divided by Z_p^2 are plotted in Fig. 8 together with the results of the IA. Shown also are the data and IA results for 2-MeV/amu F^{9+} and $H^+ + H_2$ collisions. The Z_p^2 dependence of the BEE production is thus confirmed over this range of Z_p.

In Fig. 9, we compare theoretical and experimental DDCS evaluated at $E_{lab}=E_{lab}^{max}$ for F^{9+} on H_2 and He for various projectile energies. As discussed earlier, the experimental DDCS have been normalized to the IA DDCS at E_{lab}^{max} for each E_p for $F^{9+}+H_2$. It is seen that the He data show a similar projectile-energy dependence as the H_2 data. The extracted exponential fit to the projectile-energy dependence shown in Fig. 9 was found to be

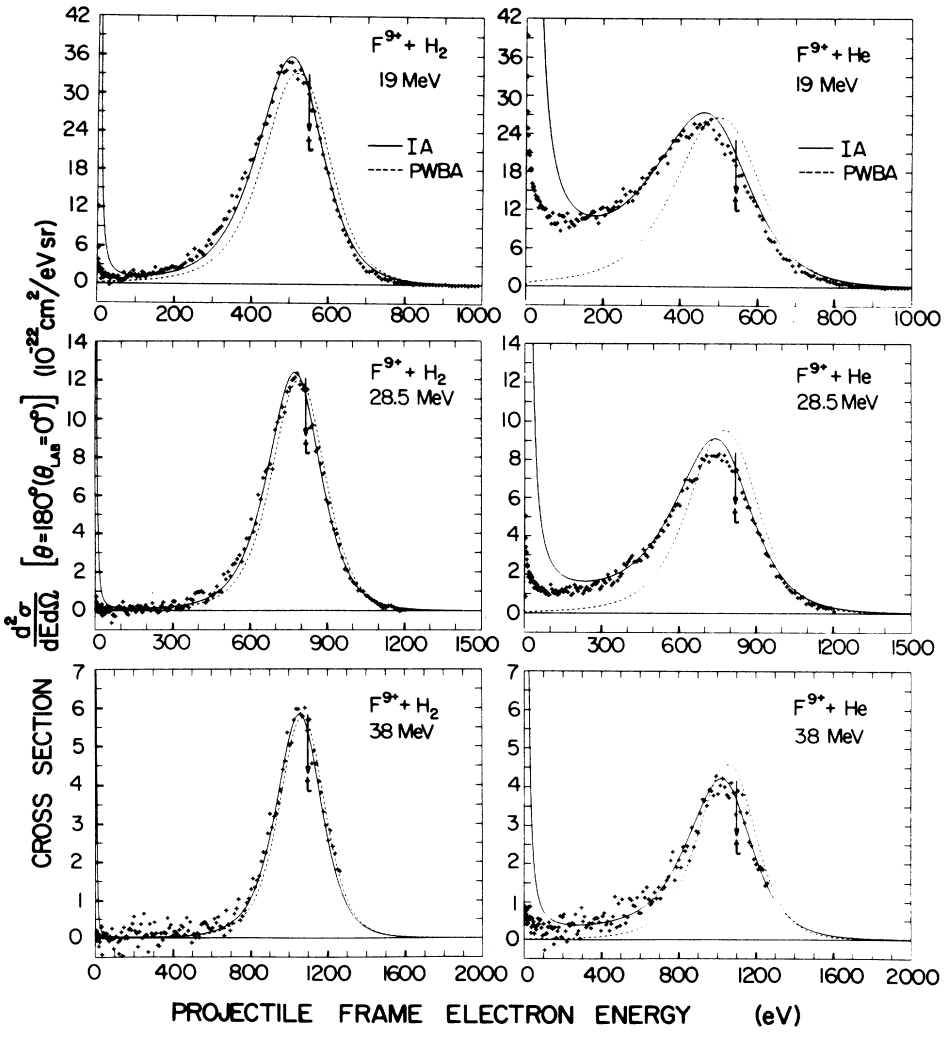

FIG. 4. BEE DDCS (projectile frame) measured at $\theta=180°$ ($\theta_{lab}=0°$ laboratory frame). Solid lines are the results of the impulse approximation (IA) as given by Eq. (6) in text. Also included for comparison (dashed lines) are the results of a plane-wave Born calculation (PWBA) (Ref. 18).

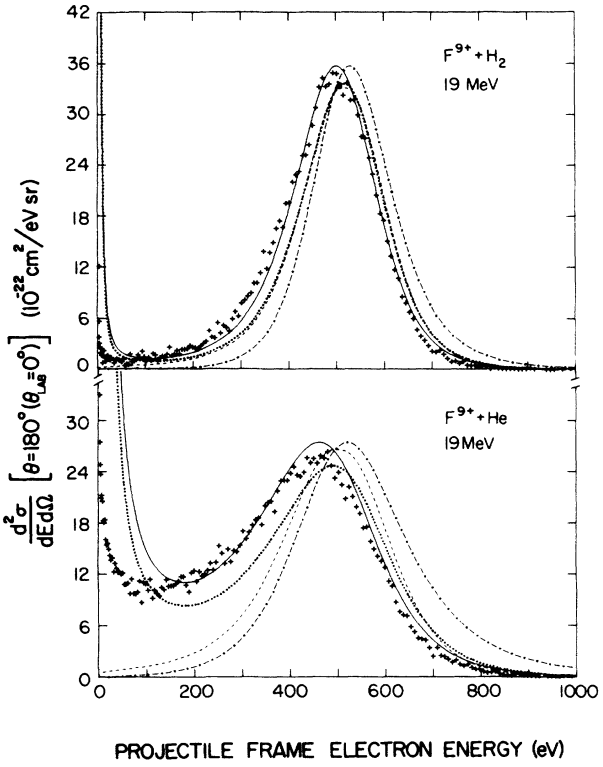

FIG. 5. Comparison of four different calculations to the measured BEE DDCS (projectile frame). Dot-dashed line: Compton profile $J(p_z)$ scaled to the IA BEE peak with $p_z(=p_{iz})$ related to E via Eq. (3). Dotted line: IA without target-electron binding energy correction [i.e., Eqs. (3) and (6) with $\lambda=0$]. Solid line: IA with the proper binding energy (see text). Dashed line: PWBA (Ref. 18).

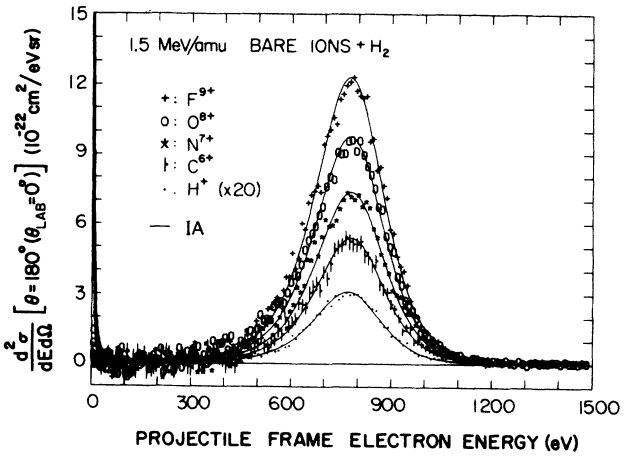

FIG. 7. BEE spectra (projectile frame) for five different bare projectiles. Typical statistical error bars are shown for the case of C^{6+}. The large error bars at the lower energies are primarily due to beam-induced background subtraction (see text) from decreasing BEE DDCS. Solid lines: full IA for each projectile. In the case of protons, both data and IA have been multiplied by 20.

$\sim E_p^{-2.6}$ for H_2 and $\sim E_p^{-2.7}$ for He targets, respectively, with 5% uncertainty. As seen from Eq. (6), an $E_p^{-2.5}$ dependence is predicted in the limit where λ and $r\rightarrow 0$.

Finally, we consider the possibility of electron capture and its effect on the BEE DDCS. Total capture for these collision systems is quite large [e.g., $\sim(5-0.3)\times 10^{-18}$ cm^2 for 1–2-MeV/amu $F^{9+}+He$],[33] however, the impact parameter relationship between capture and BEE production processes has yet to be established. In any event, any effect of capture on the BEE DDCS would manifest itself

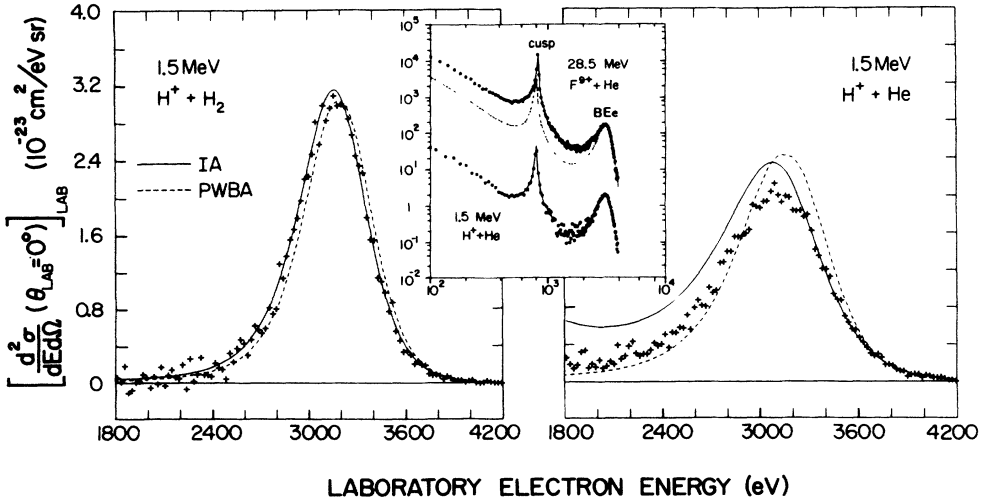

FIG. 6. BEE DDCS (laboratory frame) measured for 1.5-MeV $H^+ + H_2$ and He collisions. Solid line: full IA. Dashed line: PWBA (Ref. 18). Inset: Comparison of 1.5-MeV/amu DDCS (same units) for H^+ and $F^{9+}+He$, where the dot-dashed line is the H^+ data multiplied by Z_p^2 ($=81$).

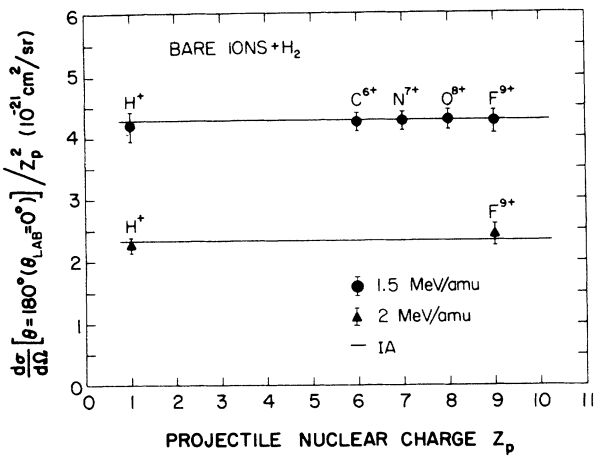

FIG. 8. Projectile charge (Z_p) dependence of BEE single differential cross sections (projectile frame). Data: solid circle (1.5 MeV/amu) and solid triangles (2 MeV/amu). Solid lines: full IA. Errors are due primarily to statistics and normalization.

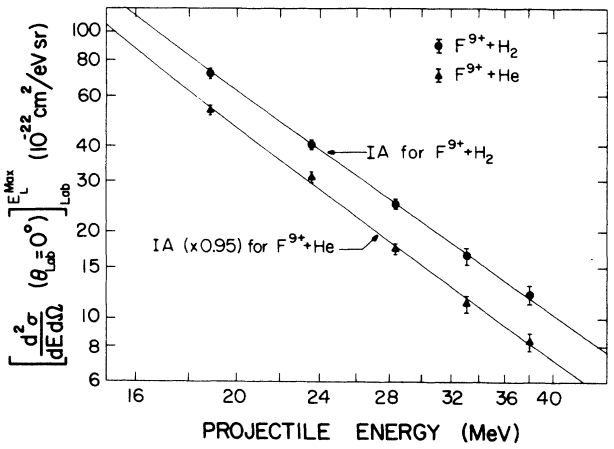

FIG. 9. Projectile energy dependence of BEE DDCS (laboratory frame) for $F^{9+}+H_2$ and He collisions. Solid lines: full IA. Closed circles and triangles: measured DDCS (at $E_{lab}=E_{lab}^{max}$) for H_2 and He targets, respectively. Errors are due mainly to statistics. The $F^{9+}+H_2$ data have been previously normalized to the IA to determine the spectrometer efficiency shown in Fig. 3 (see text).

as a deviation from the observed Z_p^2 scaling, since capture at these collision energies is known[33–36] to vary as $\sim Z_p^3$. The strong confirmation of the Z_p^2 scaling of the BEE DDCS, as shown in Fig. 8, suggests that capture can be neglected in the collision systems studied here. A similar argument can also be made about the E_p dependence of capture[35,36] ($\sim E_p^{-4.5}$) compared to that of BEE production ($\sim E_p^{-2.6}$).

VI. CONCLUSIONS

In summary, binary encounter electron (BEE) production at 0° was studied in 1–2-MeV/amu collisions of bare ions ranging from protons to F^{9+} with H_2 and He targets. At these collision energies the BEE were found to be well separated from the cusp electrons facilitating the determination of their double differential cross sections (DDCS). A description of the BEE production mechanism within an impulse approximation (IA) treatment, in which the target electrons undergo a 180° Rutherford scattering by the projectile nucleus in the projectile frame, was found to account for both the position and the shape of the measured BEE DDCS. Attempts to use the known $H^+ + Ne$ K Auger cross sections to obtain an absolute normalization led to measured DDCS that were consistently lower than the results of the IA (or PWBA at high velocities) by a factor of ~0.6. By normalizing the $F^{9+}+H_2$ data to the IA calculation we obtained an efficiency curve which reflected the expected electron-energy dependence of the detection apparatus (channeltron).

Using this efficiency we found good agreement between all the BEE data and the full IA calculation, i.e., projectile nuclear charge and energy dependence, as well as target binding energy effects. Calculated BEE DDCS using a PWBA were also compared to our data and the IA model and were found to be in good overall agreement. However, the PWBA calculation did not predict correctly the maximum or the shape of the BEE distribution for the He data.

The good overall systematic agreement of the IA and our measured DDCS suggests that the IA could provide experimentalists with a direct and relatively easy method for an *in situ* efficiency calibration of electron spectrometers at laboratory electron energies larger than about 1 keV. This would be particularly useful in characterizing Auger electron measurements in ion-atom collisions of processes such as RTE,[37] ionization, excitation and capture.

ACKNOWLEDGMENTS

We would like to acknowledge stimulating discussions with C.P. Bhalla and B.D. DePaola. This work was supported by the Division of Chemical Sciences, Office of Basic Energy Sciences, Office of Energy Research, U.S. Department of Energy.

*Present address: University of Crete and Research Center of Crete, Department of Physics, Iraklion, Greece.

[1]N. Stolterfoht, D. Schneider, R. Burch, H. Wieman, and J. S. Risley, Phys. Rev. Lett. **33**, 59 (1974).

[2]D. Berényi, in *Proceedings XV Brasov International School on Atomic and Nuclear Heavy Ion Interaction, Poiana Brasov, 1984,* edited by A. L. Berinde, I. A. Dorobantu, V. Zoran (Central Institute of Physics, Bucharest, 1986), p. 161.

[3]N. Stolterfoht, in *Structure and Collisions of Ions and Atoms,* edited by I. A. Sellin (Springer-Verlag, Berlin, 1978), pp. 155–199.

[4]M. E. Rudd and J. H. Macek, Case Stud. At. Phys. **3**, 47 (1972).

[5]G. N. Ogurtsov, Rev. Mod. Phys. **44**, 1 (1972).
[6]M. E. Rudd, L. H. Toburen, and N. Stolterfoht, At. Data Nucl. Data Tables **23**, 405 (1979).
[7]S. T. Manson, L. H. Toburen, D. H. Madison, and N. Stolterfoht, Phys. Rev. A **12**, 60 (1975).
[8]L. H. Toburen and W. E. Wilson, Phys. Rev. A **19**, 2214 (1979).
[9]T. F. M. Bonsen and L. Vriens, Physica **47**, 307 (1970).
[10]F. Drepper and J. S. Briggs, J. Phys. B **9**, 2063 (1976).
[11]P. D. Fainstein, V. H. Ponce, and R. D. Rivarola, J. Phys. B **22**, 1207 (1989).
[12]C. Kelbch, R. E. Olson, S. Schmidt, H. Schmidt-Böcking, and S. Hagmann, J. Phys. B **22**, 2171 (1989).
[13]C. P. Bhalla, Phys. Rev. Lett. **64**, 1103 (1990).
[14]T. J. M. Zouros, C. P. Bhalla, D. H. Lee, and P. Richard (unpublished).
[15]L. H. Toburen, N. Stolterfoht, P. Ziem, and D. Schneider, Phys. Rev. A **24**, 1741 (1981).
[16]P. Richard, D. H. Lee, T. J. M. Zouros, J. M. Sanders, and J. L. Shinpaugh, J. Phys. B. Lett. (to be published).
[17]D. Brandt, Phys. Rev. A **27**, 1314 (1983).
[18]Refer to Eq. (18) of Ref. 4.
[19]C. W. Woods, R. L. Kauffman, K. A. Jamison, N. Stolterfoht, and P. Richard, Phys. Rev. A **13**, 1358 (1976).
[20]L. H. Toburen, in *Proceedings of the International Conference on Inner-Shell Ionization Phenomena and Future Applications, Atlanta, Georgia, 1972,* edited by R. W. Fink, S. T. Manson, J. M. Palms, and P. V. Rao (National Technical Information Service, U.S. Department of Commerce, Springfield, VA., 1972), p. 979.
[21]D. H. Lee, T. J. M. Zouros, J. M. Sanders, J. L. Shinpaugh, T. N. Tipping, S. L. Varghese, B. D. DePaola, and P. Richard, Nucl. Instrum. Methods Phys. Res. B **40/41**, 1229 (1989).
[22]T. J. M. Zouros, D. H. Lee, and P. Richard, Phys. Rev. Lett. **62**, 2261 (1989).
[23]T. J. M. Zouros, D. H. Lee, J. M. Sanders, J. L. Shinpaugh, T. N. Tipping, S. L. Varghese, and P. Richard, Nucl. Instrum. Methods Phys. Res. B **40/41**, 17 (1989); T. J. M. Zouros, D. H. Lee, P. Richard, J. M. Sanders, J. L. Shinpaugh, S. L. Varghese, K. R. Karim, and C. P. Bhalla, Phys. Rev. A **40**, 6246 (1989).
[24]In the worst case, using the 19-MeV F^{9+} + He capture cross section from Ref. 33, a gas cell length of 10 cm, and a target gas pressure of 40 mTorr, the capture probability is 7%. Neutralization from such capture would change the integrated current by less than 1%.
[25]J. S. Lee, J. Chem. Phys. **66**, 4906 (1977).
[26]N. Stolterfoht, Phys. Rep. **146**, 315 (1987).
[27]R. Mann, S. Hagmann, and L. Weitzel, Nucl. Instrum. Methods Phys. Res. B **34**, 403 (1988).
[28]N. Stolterfoht, in *Fundamental Processes in Energetic Atomic Collisions,* Vol. 103 of *NATO Advanced Study Institute, Series B: Physics,* edited by H. O. Lutz, J. S. Briggs, and H. Kleinpoppen (Plenum, New York, 1983), p. 295.
[29]L. H. Toburen, Phys. Rev. A **3**, 216 (1971).
[30]J. P. Macau, J. Jamar, and S. Gardier, IEEE Trans. Nucl. Sci. **NS-23**(6), 2049 (1976).
[31]F. Bordoni, Nucl. Instrum. Methods **97**, 405 (1971).
[32]R. L. Arnoldy, P. O. Isaacson, D. F. Gats, and L. W. Choy, Rev. Sci. Instrum. **44**, 172 (1973).
[33]T. R. Dillingham, J. R. Macdonald, and P. Richard, Phys. Rev. A **24**, 1237 (1981).
[34]D. Brandt, Nuclear Instrum. Methods **214**, 93 (1983).
[35]A. S. Schlachter, J. W. Stearns, W. G. Graham, K. H. Berkner, R. V. Pyle, and J. A. Tanis, Phys. Rev. A **27**, 3372 (1983).
[36]A. S. Schlachter, J. W. Stearns, K. H. Berkner, M. P. Stöckli, W. G. Graham, E. M. Bernstein, M. W. Clark, and J. A. Tanis, in *Abstracts of the Fifteenth International Conference on the Physics of Electronic and Atomic Collisions, Brighton, 1987,* edited by J. Geddes, H. B. Gilbody, A. E. Kingston, C. J. Latimer, and H. J. R. Walters (Queen's University, Belfast, 1987), p. 505.
[37]We have already used this method for determining the absolute spectrometer efficiency in our recent RTEA study of Ref. 14. Using the efficiency of Fig. 3, it was found that theory in Ref. 13 is in good agreement with our renormalized RTEA single differential cross sections in Ref. 14.